Ocean Engineering 280 (2023) 114778

Contents lists available at ScienceDirect

Ocean Engineering

journal homepage: www.elsevier.com/locate/oceaneng

Contribution of the rotational kinematic interaction to the seismic response of monopile-supported offshore wind turbines

Cristina Medina *, Guillermo M. Álamo, Luis A. Padrón

Instituto Universitario de Sistemas Inteligentes y Aplicaciones Numéricas en Ingeniería (SIANI), Universidad de Las Palmas de Gran Canaria, Spain

ARTICLE INFO

Keywords:
Offshore wind turbines
Soil–structure interaction
Seismic loading
Monopile
Structural response

ABSTRACT

This paper presents a study on the role of kinematic interaction effects on the seismic response of large monopile-supported offshore wind turbines. For this purpose, a finite element substructuring model is used to analyse the behaviour of three reference wind turbines with rated powers of 5, 10 and 15 MW founded on several soil profiles and subjected to different accelerograms. The foundation response is computed through a continuum model which includes soil–structure interaction. The effects of inertial and kinematic soil–structure interaction on the system seismic response is evaluated also through comparisons with results corresponding to the infinitely rigid base condition. It is found that neglecting kinematic interaction factors could lead to underestimate the seismic response of large monopile-supported offshore wind turbines. The rotational kinematic interaction factor is shown to increase the OWTs seismic response.

1. Introduction

The wind power expansion around the world is leading to consider locations with increasing seismic risk as potential sites for the installation of Offshore Wind Turbines (OWTs). Besides, the wind energy industry is developing increasingly larger and powerful units which implies a greater impact of their potential failure. Therefore, an appropriate design of these structures including seismic excitations is gaining relevance.

Although only marginal attention was paid to seismic analysis in the main standards and design guidelines for this type of structures (DNV, 2002, 2014; IEC, 2005, 2009), a new recommended practice (DNV, 2021) has been recently published which also confirms the current needs of guidance for the seismic design of OWTs. However, further investigation is required to understand the seismic response of these structures and the seismic excitations acting on turbines with increasing sizes and rated powers, as those that are currently installed.

The analysis of the existing literature reveals that many researchers have already shown that soil–structure interaction (SSI) effects modify the dynamic response of the system (Zaaijer, 2006; Damgaard et al., 2014; Bisoi and Haldar, 2015; Galvín et al., 2017; Álamo et al., 2018; Padrón et al., 2022). However, as pointed out by Kaynia (2021), very little research effort has been put into foundation kinematic response of these type of structures, even if this is a crucial information to conduct seismic response analysis based on the substructuring approach. Most of the reported research on the earthquake response of these structures including soil–structure interaction is related to inertial interaction. Kaynia (2021) used a rigorous numerical model to compute rotational and horizontal kinematic responses at the head of a monopile embedded in different soil profiles and supporting the NREL 5-MW offshore wind turbine. This study highlighted the relevance of the consideration of kinematic interaction in the SSI seismic analysis of OWTs. Up to the authors' knowledge, there are few studies (e.g., Yang et al., 2020; Yan et al., 2021; Bhattacharya et al., 2021; Medina et al., 2021; Padrón et al., 2022) in the scientific literature addressing the seismic behaviour of larger OWTs. Medina et al. (2021) confirmed the importance of considering the seismic excitation in the design of large monopile-supported OWTs when they are installed in seismic prone areas. This study showed that the seismic response computed considering SSI effects could even duplicate that obtained for the rigid base assumption, which corroborates the importance of including the soil-foundation system in the analysis of the seismic response of the OWT system.

This paper aims at contributing to elucidate the role of kinematic interaction effects on the seismic response of large OWTs supported on monopiles. For this purpose, the behaviour of three reference wind turbines with rated powers of 5, 10 and 15 MW founded on five soil profiles and subjected to ten accelerograms extracted from the PEER Ground Motion Database (Pacific Earthquake Engineering Research Center (PEER), 2021) is analysed. The foundation response is computed through a continuum model (Álamo et al., 2016) which includes SSI.

* Corresponding author.
E-mail addresses: cristina.medina@ulpgc.es (C. Medina), guillermo.alamo@ulpgc.es (G.M. Álamo), luis.padron@ulpgc.es (L.A. Padrón).

https://doi.org/10.1016/j.oceaneng.2023.114778
Received 5 October 2022; Received in revised form 22 April 2023; Accepted 6 May 2023
Available online 27 May 2023

Table 1
Definition of the set of OWTs and monopiles used in the present study.

OWT	NREL 5 MW	IEA-10.0-198-RWT	IEA-15-240-RWT
Rating (MW)	5	10	15
Rotor–Nacelle-Assembly mass (t)	350	686	1017
Tower height (m)	90	119	150
Rotor diameter (m)	126	198	240
Tower top diameter (m)	3.87	5.5	6.5
Tower bottom diameter (m)	6.0	8.3	10.0
Tower top thickness (m)	0.0190	0.0316	0.0240
Tower bottom thickness (m)	0.0270	0.0711	0.0365
Density of steel (kg/m^3)	8500	8500	7850
Pile diameter (m)	6.0	9.0	10.0
Pile thickness (m)	0.0600	0.1015	0.0553
Pile embedded length (m)	36.0	42.6	45.0
Pile length over mudline (m)	20.0	30.0	30.0

Table 2
Dynamic properties of the soil deposits considered for soil profile B depending on the OWT.
Source: Extracted from (Alpan, 1970; Velarde and Bachynski, 2017; Løken and Kaynia, 2019; Gaertner et al., 2020; Padrón et al., 2022).

OWT	NREL 5 MW	IEA-10.0-198-RWT	IEA-15-240-RWT
Soil profile	layered	single layer	single layer
Type of soil	sand	sand	dense sand or gravel
Poisson's ratio	0.35	0.30	0.40
Density (kg/m^3)	2000	2000	2000
Shear wave velocity, v_s (m/s)	145.9 ($0 < z < 5$ m)	214.8 ($0 < z < \infty$)	264.5 ($0 < z < \infty$)
	175.9 ($5 < z < 14$ m)		
	209.0 ($9 < z < \infty$)		
Damping ratio (%)	5	5	5

Then, a finite element substructuring procedure (Medina et al., 2021) in the frequency domain is used to compute the seismic response of the superstructure. Results obtained under the infinitely rigid base condition are also presented in order to evaluate the effects of inertial and kinematic soil–structure interaction on the seismic response.

2. Problem definition

Three reference wind turbines are selected to conduct this study: the NREL 5 MW (Jonkman and Musial, 2010), the IEA-10.0-198-RWT (Bartolotti et al., 2019) and the IEA-15-240-RWT (Gaertner et al., 2020) wind turbines. The tower is modelled as a variable section tubular element; where the length is given by its height and the diameter and thickness are considered to vary linearly from the bottom to the top. Besides, the rotor–nacelle assembly is modelled as a punctual mass. Table 1 shows the properties corresponding to each structural system. In addition to these parameters, steel material properties are assumed for the tower and monopile: Young's modulus 210 GPa and Poisson's ratio 0.25. A material hysteretic damping ratio of 2% is considered. The three OWTs are supported on monopiles which are assumed to be embedded in five different soil profiles, labelled as B, H, L10, L20 and L30. Table 2 shows the material properties of soil profiles B, which correspond to the media used in the original papers that defined the monopile supporting structure for each OWT (see Padrón et al., 2022). On the other hand, Table 3 presents the dynamic properties of profiles H, L10, L20 and L30, for which a Poisson'os ratio 0.49 is considered in order to represent the saturated media.

In order to quantify the influence of considering the SSI effects when analysing the structural response, results for the infinitely rigid base assumption are also presented. Table 4 shows the natural frequencies (f_1 and f_2) and damping coefficients (ξ_1 and ξ_2) for the first two modes of vibration of the studied systems. The characteristic reductions in the natural frequencies and increments in damping due to the soil–structure interaction effects are observed in the results.

Table 3
Dynamic properties of soil deposits H and LX.

	Profile H	Profile LX
Soil profile	single layer	layered
Type of soil	sand	sand
Poisson's ratio	0.49	0.49
Density (kg/m^3)	2000	2000
Shear wave velocity, v_s (m/s)	200 ($0 < z < \infty$)	140 ($0 < z < X$ m)
		220 ($X < z < \infty$)
Damping ratio (%)	5	5

The seismic response of the system is computed by assuming ten different accelerograms extracted from the PEER Ground Motion Database (Pacific Earthquake Engineering Research Center (PEER), 2021). These acceleration signals have been selected from different earthquakes measured in stations located over soils whose mean shear wave velocities $V_{s,30}$ are within the range from 190 to 220 m/s. For reproducibility's sake, Table 5 shows the following information of the considered accelerograms: Record Sequence Number (RSN) of the database, direction with respect to the north of the horizontal component used, name and year of the earthquake event, name of the measuring station and its mean shear wave velocity, and the maximum ground acceleration $a_{g,\max}$ of the signal. A graphical representation of the normalised accelerograms corresponding to the seismic signals used in this study is provided in Fig. 1 together with their normalised pseudo-spectral accelerations (PSA). A superimposed grey line is used to represent the mean PSA of the ten seismic signals.

The measured acceleration signals are assumed to correspond to the free field motion at surface level. In order to compare the results of the

Table 4
Dynamic properties for the first and second modes of the studied systems.

OWT	Property	Rigid base	Profile B	Profile H	Profile L10	Profile L20	Profile L30
5 MW	f_1 (Hz)	0.256	0.239	0.241	0.239	0.238	0.238
	ξ_1 (%)	2.00	2.11	2.09	2.11	2.12	2.12
	f_2 (Hz)	2.28	1.94	1.99	1.93	1.93	1.92
	ξ_2 (%)	2.00	3.03	2.63	3.15	3.72	3.66
10 MW	f_1 (Hz)	0.279	0.258	0.257	0.254	0.253	0.253
	ξ_1 (%)	2.00	2.13	2.13	2.15	2.17	2.17
	f_2 (Hz)	1.77	1.50	1.49	1.44	1.43	1.43
	ξ_2 (%)	2.00	2.91	3.02	3.45	4.59	4.80
15 MW	f_1 (Hz)	0.163	0.154	0.153	0.152	0.151	0.151
	ξ_1 (%)	2.00	2.06	2.09	2.11	2.12	2.12
	f_2 (Hz)	1.37	1.23	1.21	1.18	1.18	1.18
	ξ_2 (%)	2.00	2.22	2.42	2.57	2.92	3.12

Table 5
Information about the accelerograms used in this study.
Source: (Pacific Earthquake Engineering Research Center (PEER), 2021).

RSN	Dir. (°)	Event name	Year	Station name	$V_{s,30}$ (m/s)	$a_{g,\max}$ (g)
26	271	Hollister-01	1961	Hollister City Hall	199	0.11
192	180	Imperial Valley-06	1979	Westmorland Fire Sta	194	0.11
462	271	Morgan Hill	1984	Hollister City Hall	199	0.07
721	0	Superstition Hills-02	1987	El Centro Imp. Co. Cent	192	0.36
777	180	Loma Prieta	1989	Hollister City Hall	199	0.22
1114	0	Kobe Japan	1995	Port Island (0 m)	198	0.35
1317	0	Chi-Chi Taiwan	1999	ILA013	199	0.15
2720	0	Chi-Chi Taiwan-04	1999	CHY056	193	0.07
5991	320	El Mayor-Cucapah Mexico	2010	El Centro Array 10	203	0.36
6890	10	Darfield New Zealand	2010	Christchurch Cashmere High School	204	0.23

different earthquakes, the system response is presented divided by the maximum ground acceleration of each signal.

3. Methodology

The seismic response of each OWT and supporting monopile is computed through the frequency-domain finite element substructuring simplified model described in detail in Medina et al. (2021) in which turbine tower and the section of the monopile above mudline are modelled using beam finite elements (see Fig. 2), while soil-foundation interaction is represented through the well-known approach (Wolf, 1985) of impedance functions to model the soil-foundation system reactions, and foundation input motions to model kinematic interaction (see Fig. 2) produced by the presence of the monopile.

On the one hand, the hollow tower and monopile are represented through two-noded Bernoulli's beam finite elements. Distributed inertial properties are considered for the tower and monopile elements, while the additional mass introduced by the rotor–nacelle assembly is considered as a punctual mass at the top node.

On the other hand, the soil-foundation system response is modelled through impedance functions and kinematic interaction factors computed with a previously developed continuum model (Álamo et al., 2016, 2021) for the dynamic analysis of pile foundations that allows to consider complex soil profiles. This model is based on the use of the integral expression of the reciprocity theorem together with specific Green's functions for the layered half space for representing the soil behaviour, including its radiation and material damping. Thus, linear-elastic behaviour is assumed for the whole soil-foundation-structure system.

The horizontal K_{HH}, rocking K_{RR}, and horizontal-rocking cross-coupled K_{HR} impedance functions represent the stiffness and damping of the different vibration modes of the soil-foundation system. The lateral I_u and rotational I_φ kinematic interaction factors quantify the filtering effect due to the presence of the monopile in the soil in terms of the ratio between the pile head displacement or rotation with respect to the free field motion u_{ff}. To compute them, the problem of a single pile (without superstructure) subjected to an incident S-wave is addressed.

The dynamic response of the whole system is characterised through the corresponding Frequency Response Functions (FRFs) relating the quantities of interest to the seismic waves and acting loads. Then, the seismic response in time domain for each accelerogram is computed using the frequency-domain method (Chopra, 2017) through the use of the Fast Fourier Transform.

4. Results

4.1. Foundation behaviour

4.1.1. Impedance functions

The real parts of the soil-foundation translational K_{HH}, rotational K_{RR} and cross-coupled horizontal-rocking K_{HR} impedance functions for the five soil profiles considered in this study are represented with different colours in Fig. 3. Imaginary parts are not shown for the sake of brevity. Results corresponding to the monopile supporting each one of the OWTs considered in this work (5 MW, 10 MW and 15 MW) are depicted in columns. The horizontal axis represents the excitation frequency f. Note that the same scale is used for all graphs that correspond to the same vibration mode regardless the monopile size.

As expected, and given the properties of foundations and soils provided in Tables 1–3, the stiffness of the soil-foundation system for profile B (for which it has been designed) increases with the rated power of the turbine it belongs to. On the other hand, for the common homogeneous profile (H), the monopile of the 5 MW system is, as expected, the most flexible one, while the foundations corresponding

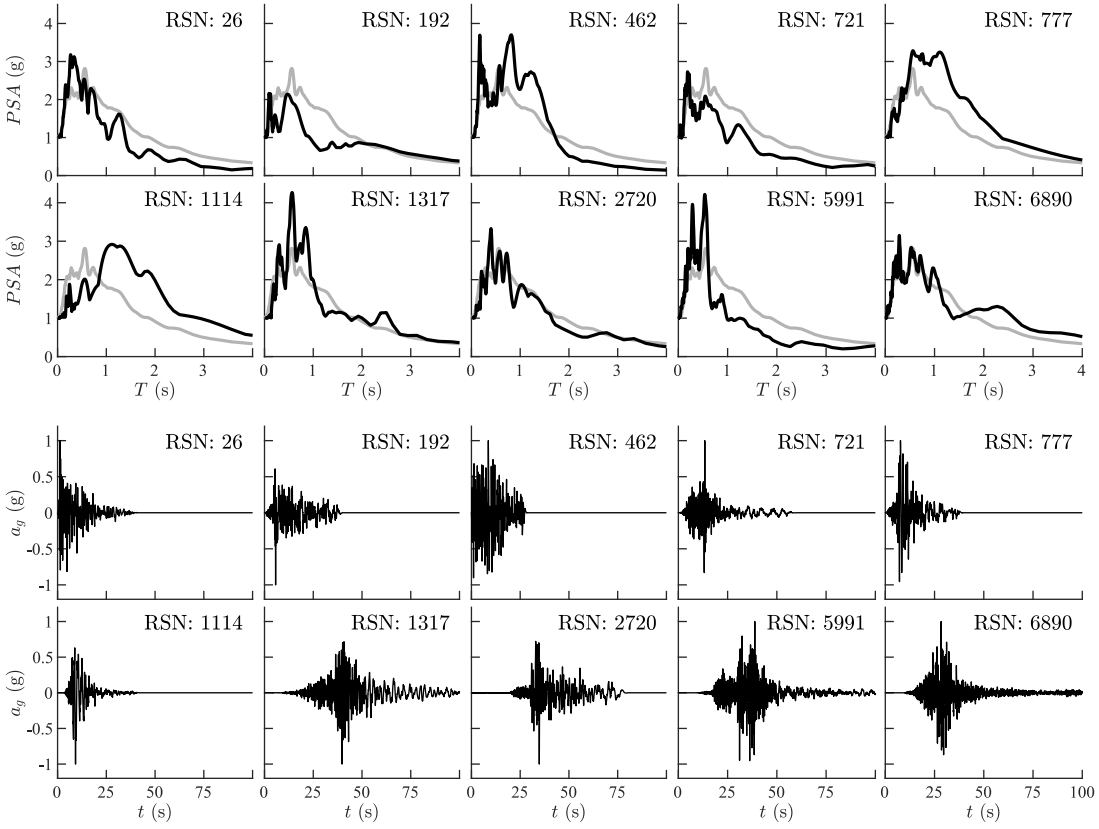

Fig. 1. Normalised pseudo-spectral accelerations (PSA) and ground acceleration (a_g) of the seismic signals used in this study.

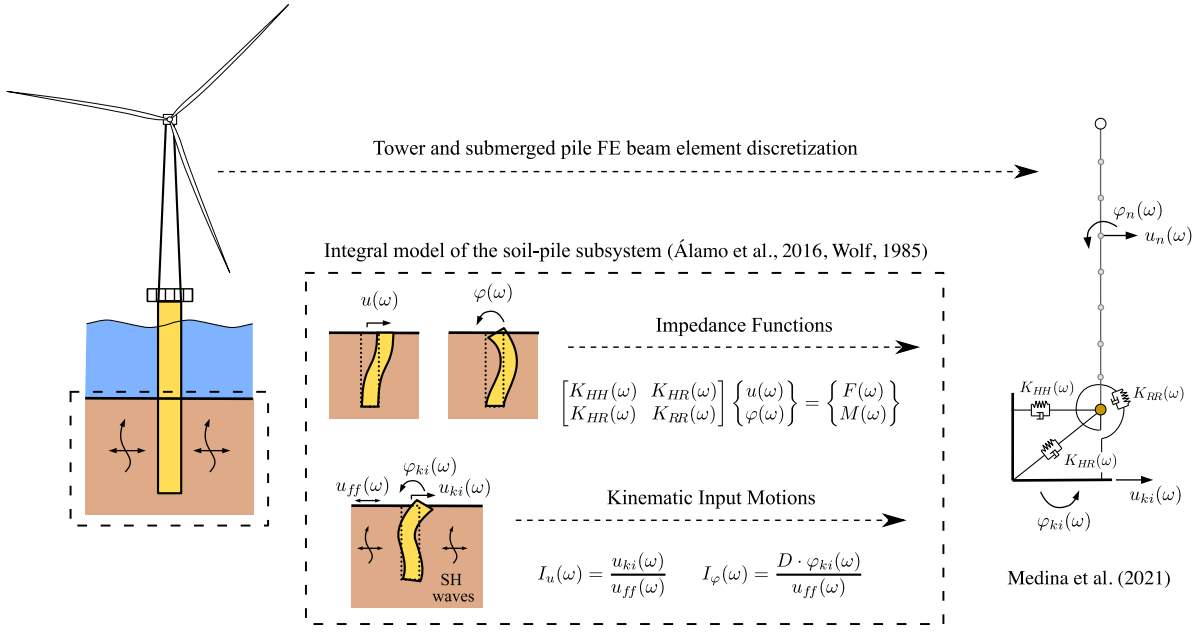

Fig. 2. Frequency-domain finite element substructuring simplified model used in this work.

to the 10 and 15 MW turbines present similar horizontal stiffness. However, for the rotational and cross-coupled terms, the monopile of the 10 MW generator is the most rigid foundation. This is due to its large thickness compared with the 15 MW pile (see Table 1), which affects more to rotational modes. The relation between the homogeneous and base profile should be carefully taken into account when analysing the structural response: profile H is stiffer (5 MW), similar (10 MW) or softer (15 MW) than profile B depending on the system. On the other hand, comparing the impedance functions obtained for the three considered layer profiles (L10, L20 and L30), they are similar or smaller than the ones obtained for the base or homogeneous profiles. As expected, the foundation becomes more flexible if the height of the upper (soft) layer increases, being larger the differences between the L10 and L20 profiles than the ones between the L20 and L30 profiles. The influence of the definition of the soil profile is larger for the horizontal impedance term. On the contrary, the rocking impedance

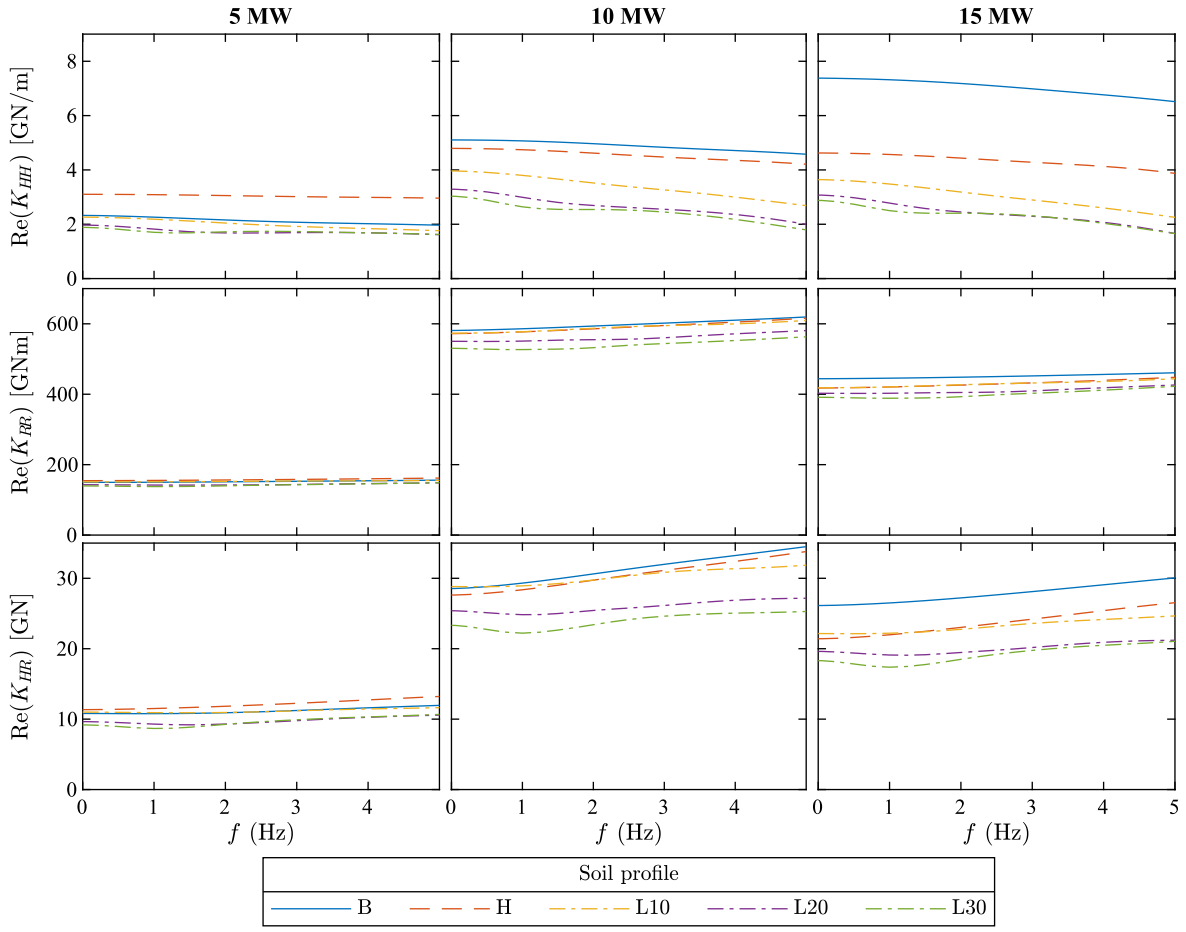

Fig. 3. Real part of the translational K_{HH}, rotational K_{RR} and crossed-coupled horizontal-rocking K_{HR} impedance functions obtained for the different soil profiles considered in this study.

is less affected by the assumed soil profile, especially in the case of the 5 MW system.

4.1.2. Kinematic interaction factors

The filtering of the ground motion produced by each foundation is represented in Fig. 4 in terms of the real and imaginary parts of the kinematic interaction factors corresponding to the different monopiles supporting the OWTs under study. Results for the five soil profiles considered in this work are represented with different colours in a superimposed manner.

The relation between profiles B and H depends on the system. A more pronounced filtering effect is observed for profile H, except in the case of the 5 MW OWT. The greatest filtering occurs for layered profiles (L10, L20 and L30). In fact, for the kinematic interaction, the differences between the results of the layered profiles are more evident than for the impedance functions.

The lateral kinematic terms show that no filtering effect is produced below 2 Hz, range in which the two first modes of the tower-monopile system are located (see Section 4.2). Also, for these small frequencies, only a slight amplification of the ground motion, characteristic to the free-head pile kinematic response, is observed. This implies that considering this term would have a minor impact on the system seismic response. For higher frequencies ($f > 2$ Hz), the filtering effect of the foundation increases, as well as the phase difference between the pile head and soil free field motions. This happens at lower frequencies for the softer profiles (L30, L20, L10).

On the other hand, the rotational kinematic interaction factor shows induced pile head rotation for almost all the studied frequency range. For the frequency range 0.5–2 Hz, the rotation presents a real non-zero value and its imaginary part is zero, which denotes that the movement is in phase with the soil. The negative sign is derived from the sign criteria used in the model. For frequencies over approximately 2 Hz, the imaginary component of the rotational kinematic interaction factors shows the phase difference with respect to the soil free field motion that was already commented for the lateral movement. Regarding the effect of the soil profile, larger rotations at smaller frequencies arise for the more flexible soils.

4.2. Frequency response functions

For the purpose of illustrating the influence of considering kinematic interaction on the structural response, Fig. 5 presents different Frequency Response Functions for the tower top acceleration $a_{top}/a_{g,max}$ (right column) and the bending moment at the mudline level $M_{base}/a_{g,max}$ (left column) in the frequency range including the first two modes for the three wind turbines under study founded on soil profile B.

In order to identify the contribution of the different variables involved in the SSI problem in each case, three scenarios are considered in addition to that corresponding to the assumption of rigid base condition (black solid line): (a) the response obtained when taking only inertial interaction into account, i.e. without including the filtering effect of the kinematic interaction ($I_u = 1$ and $I_\varphi = 0$), is represented with a blue solid line; (b) the contribution of the translational kinematic interaction term I_u to the total response is depicted with a green dashed line; and finally, (c) the results computed including both terms of kinematic interaction, I_u and I_φ, are plotted with a red solid line. In order to provide supplementary information regarding the energy of

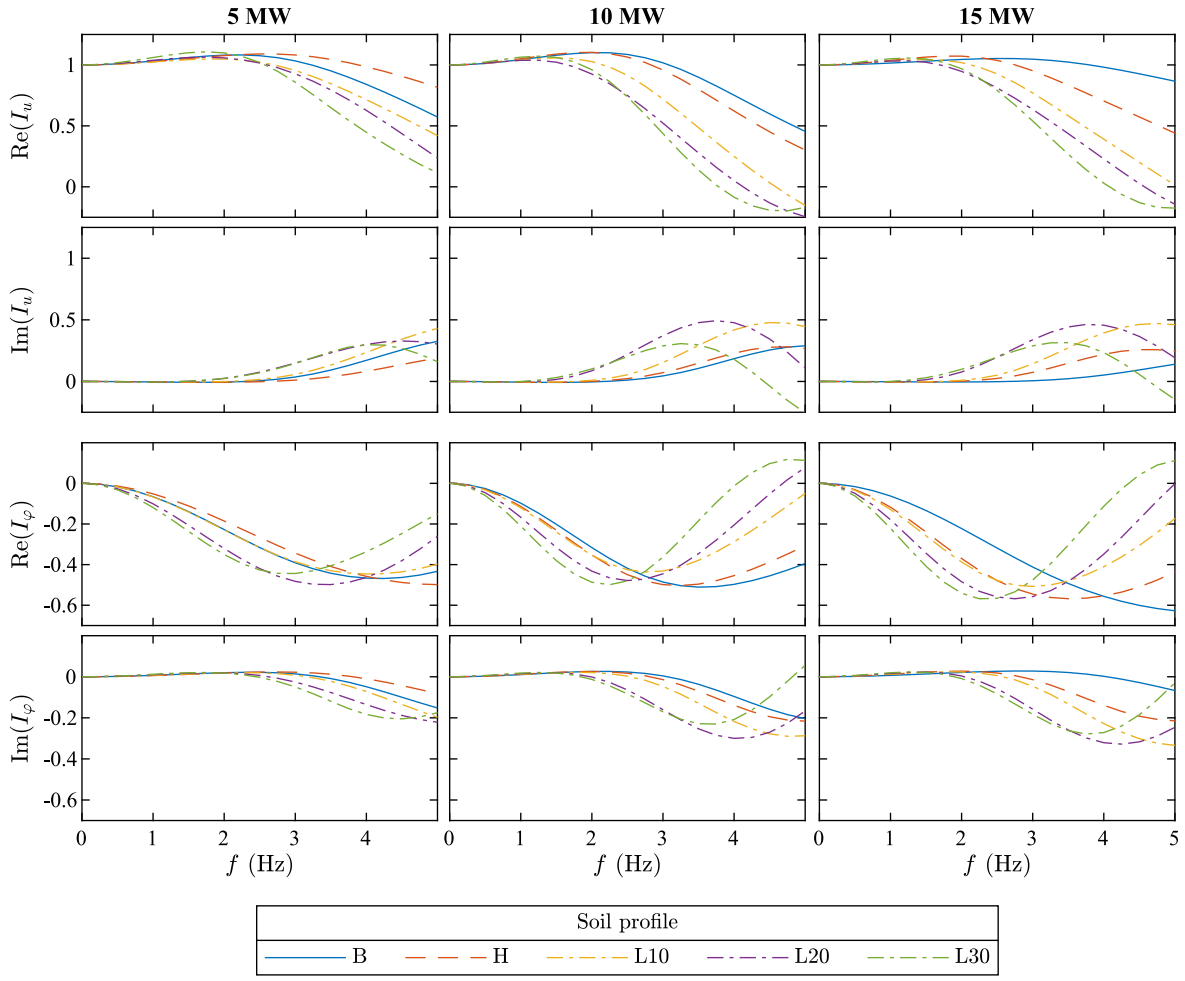

Fig. 4. Real and imaginary parts of the translational (I_u) and rotational (I_φ) kinematic interaction factors obtained for the different soil profiles considered in this study.

the seismic signals selected for this study, the mean pseudo-spectral acceleration (PSA) of these ten seismic signals is displayed as a grey shaded area in each chart.

A remarkable increase of the response amplitude is observed as a consequence of considering the rotational kinematic interaction factor, specially on the second mode, which has a significant role on the seismic response in view of the shape of the mean PSA of the signals considered in this work. No relevant changes with respect to the SSI-inertial response are observed when only the translational kinematic interaction factor is included. It is worth mentioning that the frequency at which the first mode of the 15 MW OWT occurs is lower than that corresponding to the first mode of the 5 MW and 10 MW wind turbines, which explains a reduction of its seismic response. Similar conclusions can be drawn from the Frequency Response Functions corresponding to the different soil profiles considered in this work.

4.3. Structural seismic response

The trends observed in the frequency response functions provided in Section 4.2 can also be seen in Fig. 6 that shows, as an example, time histories of the tower top acceleration (top) and the bending moment at the mudline level (bottom) for the 15 MW OWT founded on soil profile B and subjected to the seismic signal with RSN: 1317. Both variables are presented divided by the maximum ground acceleration $a_{g,max}$. The relevant role of the rotational kinematic interaction factor is shown to be consistent over all the significant duration of the earthquake ground motion. It is worth mentioning that the contribution of both kinematic interaction factors, previously represented in frequency, has an additive effect since both are virtually in phase.

In order to show the contribution of kinematic soil–structure interaction effects on the seismic response of the three reference OWTs under study, the following sections present an analysis of tower top accelerations and bending moments at seabed.

For the purpose of determining the maximum response value reached in each case of study, the peak value of the time response is computed for each one of the ten accelerograms considered in this work. Furthermore, in order to check whether the conclusions drawn from the analysis of the response peak value can be extrapolated to all the time signal, the root mean square (RMS) value of the response in the significant duration of each seismic signal is also calculated. The common D_{a5-95} significant duration (see, e.g. Dobry et al., 1978; Kamiyama, 1984) is considered, which is defined as the time interval between 5%–95% of the Arias intensity (Arias, 1970). The mean value of the results in terms of peak value and RMS value for the ten aforementioned accelerograms is represented in Figures from 7 to 10 and analysed in the following sections.

Different colour bars are used to represent results either for the five soil profiles defined in Section 2 in Figs. 7 and 9, or for the different scenarios in Figs. 8 and 10, as indicated in the corresponding legend. The results corresponding to the assumption of rigid base condition are displayed in black as reference results to compare the different scenarios. For the purpose of analysing the contribution of the translational and rotational kinematic interaction factors, in Figs. 7 and 9 each row shows results for the three scenarios already described in Section 4.2.

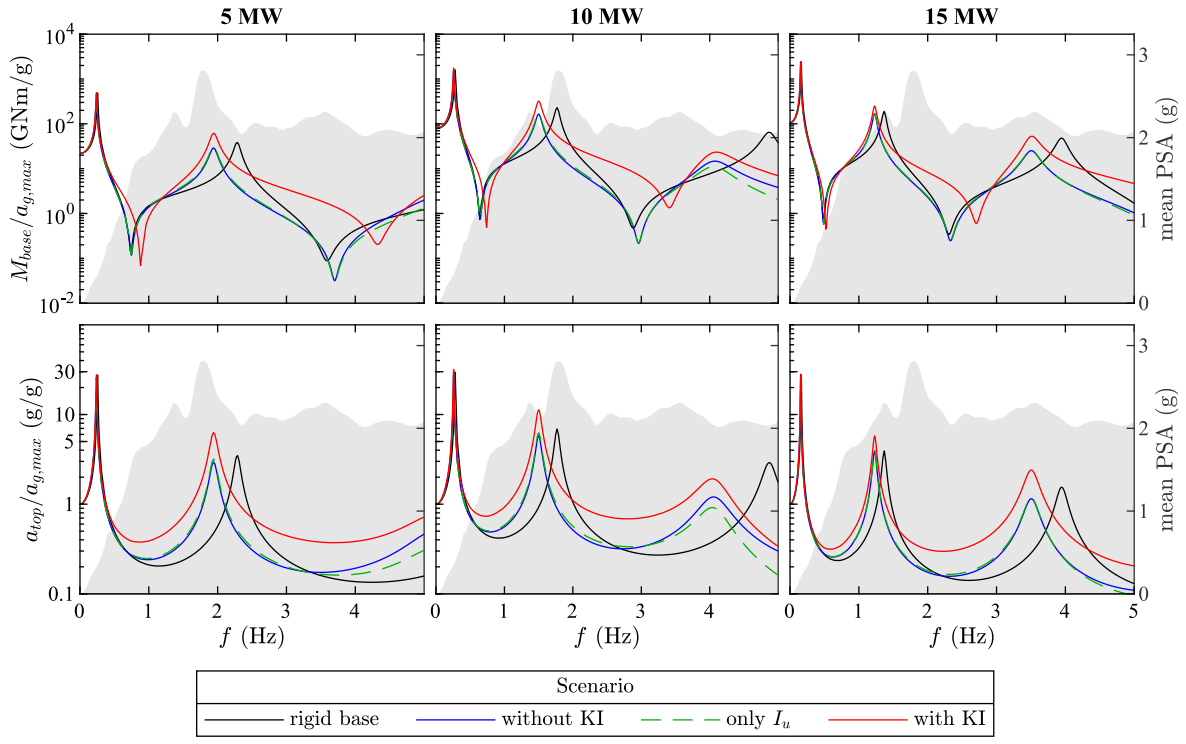

Fig. 5. Frequency Response Functions for the bending moment at the mudline level ($M_{base}/a_{g,max}$) and the acceleration at the tower top ($a_{top}/a_{g,max}$) over mean pseudo-spectral acceleration (represented as a grey shaded area to be read on the right axis) of the 10 seismic signals used in this study. Soil profile B.

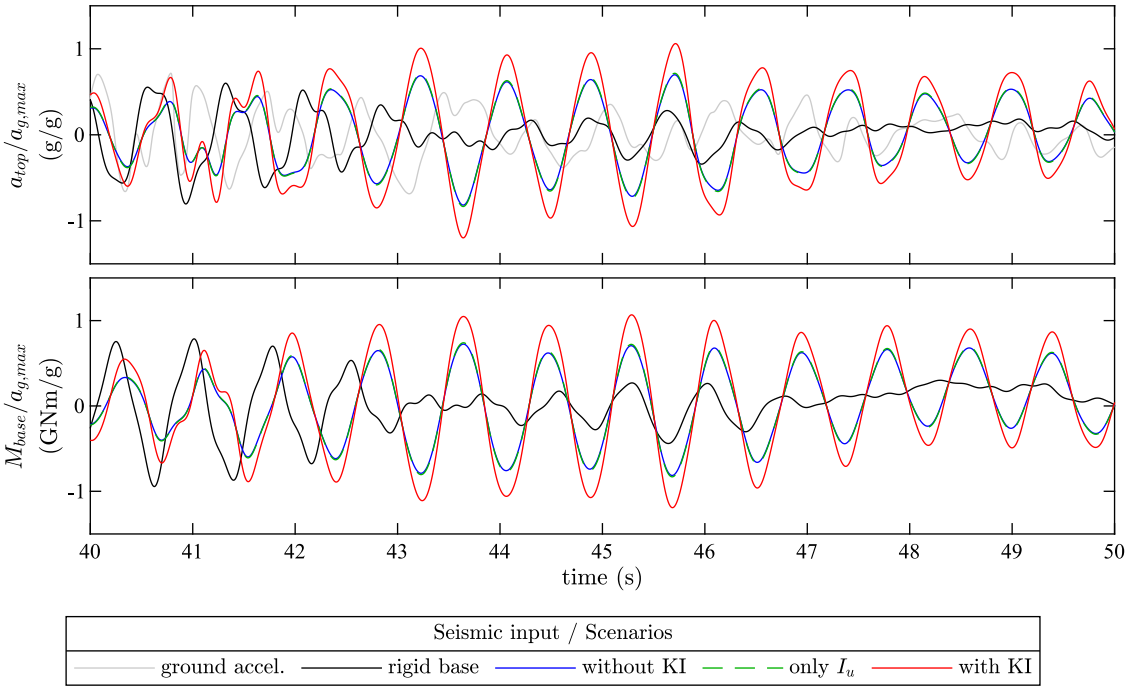

Fig. 6. Time histories of the tower top acceleration ($a_{top}/a_{g,max}$) and the bending moment at the mudline level ($M_{base}/a_{g,max}$) for the 15 MW OWT founded on soil profile B and subjected to the seismic signal with RSN: 1317.

4.3.1. Tower top accelerations

Fig. 7 presents the mean peak value and the mean RMS value of the tower top acceleration normalised with the peak acceleration of the corresponding seismic excitation ($a_{top}/a_{g,max}$) computed for the ten seismic signals considered in this work. The same trends are observed for both variables.

The highest response at the tower top is achieved for the 10 MW wind turbine, regardless of the soil profile considered and independently of the assumptions adopted for kinematic soil–structure interaction. As can be seen in Fig. 5, the first natural frequency in the case of the 15 MW wind turbine is lower than that corresponding to the 10 MW wind turbine which, in view of the shape of the mean PSA spectra

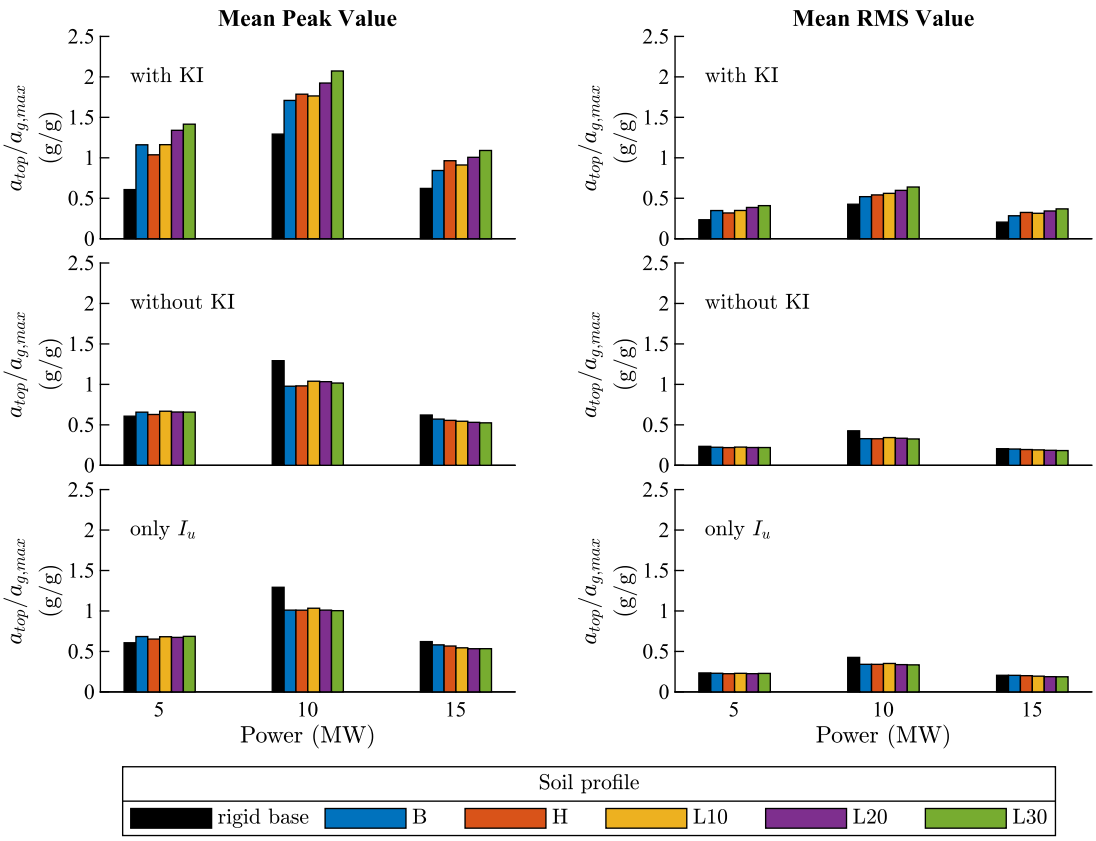

Fig. 7. Mean peak and root mean square (RMS) tower top accelerations for the five different soil profiles used in this study.

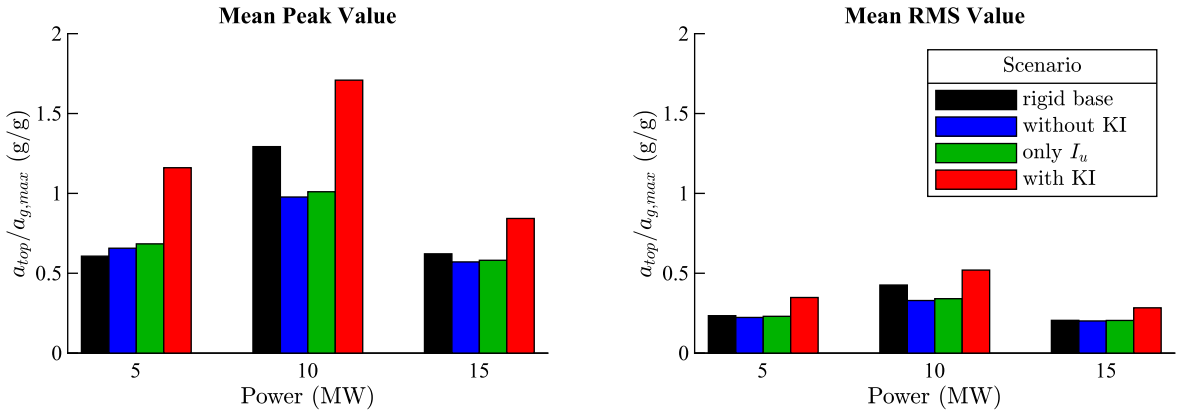

Fig. 8. Mean peak and root mean square (RMS) tower top accelerations for the different assumptions related to kinematic interaction made in this study. Soil profile B.

for the ten seismic signals used in this study, contributes to reduce its seismic response. No remarkable differences can be appreciated between results obtained without considering kinematic interaction and those computed including only the translational kinematic interaction factor. However, clear differences can be appreciated between the results obtained when both kinematic interaction factors are included and those computed considering only inertial interaction. Therefore, these differences are mainly attributed to the inclusion of the rotational kinematic interaction factor which has a significant influence on the variable under study. In fact, results increase from about 50% up to 106%, depending on the turbine and soil profile under study, when the rotational kinematic factor is taken into account. This conclusion is coherent with the analysis of the kinematic interaction factors presented in Section 4.1.2.

The variation of the soil profile has shown no relevant effects neither when only inertial interaction is included nor when the translational kinematic interaction factor is considered. However, if the rotational kinematic interaction term is taken into account, remarkable differences are detected when comparing results corresponding to different soil profiles. Higher mean peak values are reached when the monopile is embedded in a softer soil profile, experiencing an increase in the order of 20% to 30%, depending on the turbine considered, when comparing results obtained for profile B with those corresponding to profile L30.

For the purpose of elucidating how kinematic interaction affects the seismic response of the superstructure, Fig. 8 depicts, in a superimposed manner, results in terms of mean peak and root mean square tower

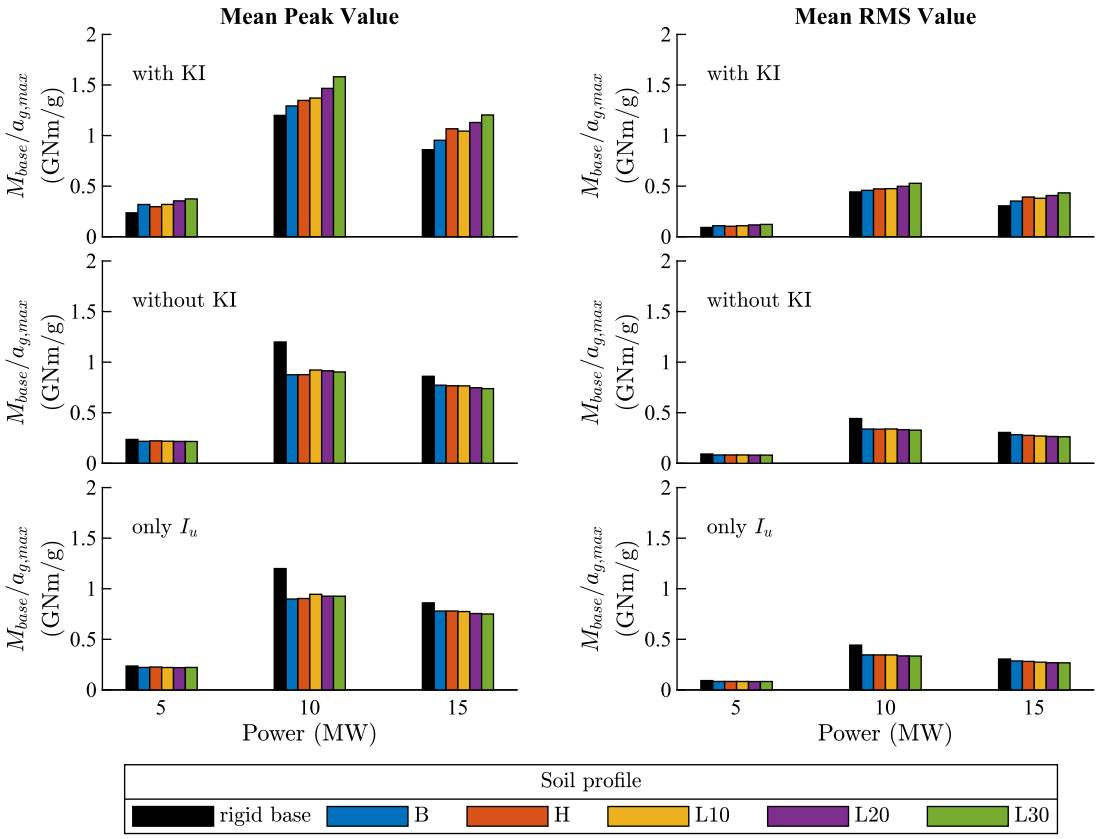

Fig. 9. Mean peak and root mean square (RMS) bending moments at the mudline level ($M_{base}/a_{g,max}$) for the five different soil profiles used in this study.

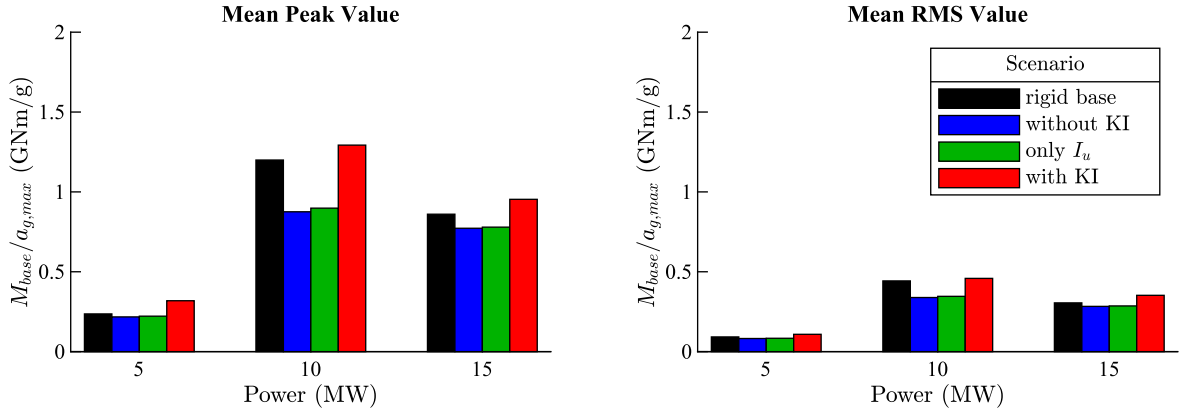

Fig. 10. Mean peak and root mean square (RMS) bending moments at the mudline level for the different assumptions related to kinematic interaction made in this study. Soil profile B.

top acceleration corresponding to three scenarios defined with different assumptions regarding the inclusion of kinematic soil–structure interaction together with those computed under rigid base condition. The three reference OWTs analysed in this work are here considered to be supported on monopiles embedded in soil profile B. Including kinematic interaction effects yields increments that go from 33% up to 90%, depending on the turbine considered, with respect to those obtained under the rigid base assumption. When comparing against those results including only inertial interaction increases from about 45% up to 71% are found. Therefore, neglecting the kinematic interaction effects would lead to underestimate the superstructure seismic response in terms of tower top acceleration.

4.3.2. Bending moments at seabed

The envelopes of maximum bending moments above mudline level for all the OWTs considered in this work reach their maximum value at the mudline level, confirming that this is a critical point in the structural design of these units. Therefore, results in terms of mean and root mean square values of the bending moments at the mudline level normalised with the peak acceleration of the corresponding seismic excitation ($M_{base}/a_{g,max}$) are plotted in Fig. 9. The first row depicts results computed including both kinematic interaction terms which exceed in all cases those obtained under rigid base assumption by from 30% to 54% depending on the turbine and soil profile considered. Note that softer soil profiles yield higher values of the response. The second

row illustrates the influence of considering only inertial soil–structure interaction, which is remarkable for the two largest wind turbines. The soil profile in which the monopile is embedded does not yield important variations in the obtained results. Finally, the third row shows that the effects of including only the translational kinematic interaction term I_u are not significant.

In order to better illustrate the importance of taking kinematic interaction into account, Fig. 10 presents results corresponding to the different assumptions adopted in this study plotted in a superimposed manner. The inclusion of both kinematic interaction terms yields greater mean peak bending moments at the mudline level than those computed under the rigid base condition. An increase from about 7.5% up to 33% can be observed depending on the turbine under study. Therefore, it is clear that neglecting these effects could lead to underestimate the seismic response of the superstructure.

5. Conclusions

This paper outlines the main conclusions drawn from a study on the contribution of kinematic interaction to the response of three large monopile-supported OWTs with rated powers of 5, 10 and 15 MW, to ten real accelerograms. To do so, a finite element substructuring simplified model in the frequency domain is used. The impedance functions and kinematic interaction factors characterising the foundation behaviour are computed through a previously developed continuum model for the layered half space that allows to consider complex soil profiles. Each monopile foundation is considered to be embedded in five different soil profiles.

Results are presented in terms of mean peak and root mean square values of the tower top acceleration and the bending moment at the mudline level normalised with the peak acceleration of the corresponding seismic excitation.

When only inertial interaction is taken into account, the seismic response values obtained are generally below those corresponding to rigid base condition.

The seismic response obtained when including only the translational kinematic interaction factor almost matches that computed when considering only inertial interaction.

The rotational kinematic interaction factor is shown to have a determinant role in the OWTs seismic response which is consistent over all the significant duration of the earthquake ground motion. In fact, a remarkable increase of the response amplitude is observed as a consequence of including the rotational kinematic interaction factor, specially on the second mode.

The variation of the soil profile has shown no relevant effects unless the rotational kinematic interaction term is taken into account. Higher mean peak values are reached when the monopile is embedded in a softer soil profile, yielding differences up to 30% for the soil profiles considered in this study.

Considering kinematic interaction effects yields response values that can almost duplicate those obtained under rigid base assumption. Therefore, neglecting them could lead to underestimate the seismic response of large monopile-supported offshore wind turbines.

CRediT authorship contribution statement

Cristina Medina: Conceptualization, Investigation, Writing – original draft, Writing – review & editing, Supervision, Project administration, Funding acquisition. **Guillermo M. Álamo:** Conceptualization, Methodology, Software, Investigation, Writing – original draft, Writing – review & editing, Visualization. **Luis A. Padrón:** Conceptualization, Methodology, Investigation, Writing – review & editing, Project administration, Funding acquisition.

Declaration of competing interest

The authors declare that they have no known competing financial interests or personal relationships that could have appeared to influence the work reported in this paper.

Data availability

Data will be made available on request.

Acknowledgements

This study was supported by the Ministerio de Ciencia e Innovación, Spain and the Agencia Estatal de Investigación (AEI) of Spain (MCIN/AEI/ 10.13039/501100011033) through research project PID2020-120102RB-I00; by Consejería de Economía, Conocimiento *y* Empleo (Agencia Canaria de Investigación, Innovación *y* Sociedad de la Información) of the Gobierno de Canarias and FEDER through research project ProID2020010025; and by Universidad de Las Palmas de Gran Canaria, Spain through research project ULPGC2018-11. This research was partially supported by ACIISI, Spain–Gobierno de Canarias and European FEDER Funds Grant EIS 2021 04.

References

Álamo, G.M., Aznárez, J.J., Padrón, L.A., Martínez-Castro, A.E., Gallego, R., Maeso, O., 2018. Dynamic soil-structure interaction in offshore wind turbines on monopiles in layered seabed based on real data. Ocean Eng. 156, 14–24.

Álamo, G.M., Bordón, J.D.R., Aznárez, J.J., 2021. On the application of the beam model for linear dynamic analysis of pile and suction caisson foundations for offshore wind turbines. Comput. Geotech. 134, 104107.

Álamo, G.M., Martínez-Castro, A.E., Padrón, L.A., Aznárez, J.J., Gallego, R., Maeso, O., 2016. Efficient numerical model for the computation of impedance functions of inclined pile groups in layered soils. Eng. Struct. 126, 379–390.

Alpan, I., 1970. The geotechnical properties of soils. Earth-Sci. Rev. 6 (1), 5–49.

Arias, A., 1970. In: Hansen, R. (Ed.), Seismic Design for Nuclear Power Plants. MIT Press, Cambridge, MA, pp. 438–483.

Bartolotti, P., Tarres, H.C., Dykes, K., Merz, K., Sethuraman, L., Verelst, D., Zahle, F., 2019. IEA Wind Task 37 on Systems Engineeringin Wind Energy – WP2.1 Reference Wind Turbines. Resreport NREL/TP-73492, International Energy Agency, https://github.com/IEAWindTask37/IEA-10.0-198-RWT.

Bhattacharya, S., Biswal, S., Aleem, M., Amani, S., Prabhakaran, A., Prakhya, G., Lombardi, D., Mistry, H.K., 2021. Seismic design of offshore wind turbines: Good, bad and unknowns. Energies 14 (12), 3496.

Bisoi, S., Haldar, S., 2015. Design of monopile supported offshore wind turbine in clay considering dynamic soil–structure-interaction. Soil Dyn. Earthq. Eng. 73, 103–117.

Chopra, A.K., 2017. Dynamics of Structures. Theory and Applications to Earthquake Engineering, 7th ed. Pearson.

Damgaard, M., Bayat, M., Andersen, L.V., Ibsen, L.B., 2014. Assessment of the dynamic behaviour of saturated soil subjected to cyclic loading from offshore monopile wind turbine foundations. Comput. Geotech. 61, 116–126.

DNV, 2002. Guidelines for Design of Wind Turbines, 2nd ed. Det Norske Veritas, Copenhagenand Wind Energy Department, Risø National Laboratory.

DNV, 2014. Design of Offshore Wind Turbine Structures. Offshore Standard DNV-OS-J101. Det-Norske Veritas AS.

DNV, 2021. Seismic Design of Wind Power Plants DNV-RP-0585. Det-Norske Veritas AS.

Dobry, R., Idriss, I.M., Ng, E., 1978. Duration characteristics of horizontal components of strong-motion earthquake records. Bull. Seismol. Soc. Am. 68 (5), 1487–1520.

Gaertner, E., Rinker, J., Sethuraman, L., Zahle, F., Anderson, B., Barter, G., Abbas, N., Meng, F., Bortolotti, P., Skrzypinski, W., Scott, G., Feil, R., Bredmose, H., Dykes, K., Shields, M., Allen, C., Viselli, A., 2020. Definition of the IEA 15 MW Offshore Reference Wind Turbine. TechreportNREL/TP-75698, International Energy Agency, https://github.com/IEAWindTask37/IEA-15-240-RWT.

Galvín, P., Romero, A., Solís, M., Domínguez, J., 2017. Dynamic characterisation of wind turbine towers account for a monopile foundation and different soil conditions. Struct. Infrastruct. Eng. 13 (7), 942–954.

IEC, 2005. 61400-1:2005 Wind Turbines - Part 1: Design Requirements. International Electrotechnical Commission.

IEC, 2009. 61400-3:2009 Wind Turbines - Part 3: Design Requirements for Offshore Wind Turbines. International Electrotechnical Commission.

Jonkman, J., Musial, W., 2010. Offshore Code Comparison Collaboration (OC3) for IEA Task 23 Offshore Wind Technology and Deployment, Techreport NREL/TP-5000-48191. Technical Report, National Renewable Energy Laboratory.

Kamiyama, M., 1984. Effects of subsoil conditions and other factors on the duration of earthquakeground shaking. In: Proceedings, 8th World Conference on Earthquake Engineering, Vol. 2. San Francisco, pp. 93–800.

Kaynia, A.M., 2021. Effect of kinematic interaction on seismic response of offshore wind turbines on monopiles. Earthq. Eng. Struct. Dyn. 50 (3), 777–790.

Løken, I.B., Kaynia, A.M., 2019. Effect of foundation type and modelling on dynamic response and fatigue of offshore wind turbines. Wind Energy 22 (12), 1667–1683.

Medina, C., Álamo, G.M., Quevedo-Reina, R., 2021. Evolution of the seismic response of monopile-supported offshore wind turbines of increasing size from 5 to 15 MW including dynamic soil-structure interaction. J. Mar. Sci. Eng. 9 (11).

Pacific Earthquake Engineering Research Center (PEER), 2021. NGA-West2 ground motion database. University of California, Berkeley, http://ngawest2.berkeley.edu/. (Accessed September 2021).

Padrón, L.A., Carbonari, S., Dezi, F., Morici, M., Bordón, J.D., Leoni, G., 2022. Seismic response of large offshore wind turbines on monopile foundations including dynamic soil–structure interaction. Ocean Eng. 257, 111653.

Velarde, J., Bachynski, E.E., 2017. Design and fatigue analysis of monopile foundations to support the dtu 10 mw offshore wind turbine. Energy Procedia 137, 3–13, 14th Deep Sea Offshore Wind R&D Conference, EERA DeepWind'2017.

Wolf, J.P., 1985. Dynamic Soil-Structure Interaction. Prentice-Hall.

Yan, Y., Li, C., Li, Z., 2021. Buckling analysis of a 10 MW offshore wind turbine subjected to wind-wave-earthquake loadings. Ocean Eng. 236, 109452.

Yang, Y., Bashir, M., Li, C., Michailides, C., Wang, J., 2020. Mitigation of coupled wind-wave-earthquake responses of a 10 MW fixed-bottom offshore wind turbine. Renew. Energy 157, 1171–1184.

Zaaijer, M., 2006. Foundation modelling to assess dynamic behaviour of offshore wind turbines. Appl. Ocean Res. 28 (1), 45–57.